A Hybrid ACA-FDM for Electromagnetic Scattering from PEC Targets

Xinlei Chen, Changqing Gu, Xiaoqiao Deng, Bingzheng Xu, Zhuo Li, and Zhenyi Niu

College of Electronic and Information Engineering
Nanjing University of Aeronautics and Astronautics, Nanjing 210016, China
gucq@nuaa.edu.cn

Abstract ─ In this paper, the adaptive cross approximation (ACA) algorithm is combined with the fast dipole method (FDM) to solve the electromagnetic scattering from perfect electric conducting (PEC) targets. In the ACA-FDM, the ACA and the FDM are employed to deal with the near-group pairs and the far-group pairs respectively. Compared with the conventional FDM, the submatrices related to the interactions of the near-group pairs are efficiently compressed by the ACA, so the ACA-FDM saves CPU time and memory requirement, when the criterion for the far-group pairs becomes stricter in order to obtain relatively high accurate solutions. Numerical results about the electromagnetic scattering from PEC targets are given to demonstrate the merits of the ACA-FDM.

Index Terms ─ Electromagnetic scattering, equivalent dipole method (EDM), fast dipole method (FDM), adaptive cross approximation (ACA).

I. INTRODUCTION

The method of moments (MoM) has been widely used to solve electromagnetic scattering problems. However, the computational complexity and memory storage of the conventional MoM which leads to a dense matrix equation are both $O(N^2)$ for matrix iterative solvers, where N is the number of unknowns. Both the matrix-fill and matrix-solve processes are expensive. Fortunately, many methods have been developed in order to overcome this problem through these years, such as multilevel fast multipole algorithm (MLFMA) [1-2], adaptive integral method (AIM) [3-4], pre-corrected fast Fourier transform (P-FFT) method [5-6] and adaptive cross approximation (ACA) algorithm [7-12].

Recently, the equivalent dipole method (EDM) [13-14] based on the commonly used Rao-Wilton-Glisson (RWG) [15] basis function has been developed to simplify the MoM impedance matrix element filling procedure. In the EDM, each RWG element is viewed as a dipole model with an equivalent moment, and the mutual impedance elements is replaced by the interactions of equivalent dipoles, which has a simple closed canonical form. However, the computational complexity and memory storage of the EDM don't change, which are still $O(N^2)$. More recently, the fast dipole method (FDM) [16-17] is proposed to mitigate this problem. Through a simple Taylor's series expansion of all the terms including R in the formulation of EDM, the FDM can achieve the separation of the field dipole and source dipole. Therefore the complexity of interactions between two far groups such as group i and j can be reduced from $O(N_i N_j)$ to $O(N_i + N_j)$, where N_i and N_j are the number of the dipoles in group i and j, respectively.

However, in order to get good solutions, the FDM has to choose stricter criterion for far-group pairs. In other words, the number of near-group pairs must increase. Although the near group interactions can be efficiently calculated by the EDM, they will still lead to rapidly increase in memory requirement and CPU time in the matrix-vector products (MVPs). In this work, the adaptive cross approximation (ACA) algorithm [8] is employed to deal with the near group interactions. The ACA is purely algebraic in nature and relatively easy to implement. Also, it does not require knowing all the impedances of

Submitted On: May 14, 2012
Accepted On: Oct. 8, 2012

submatrices. For a relatively high accuracy the hybrid ACA-FDM saves memory requirement and CPU time than the conventional FDM.

The remainder of the paper is organized as follows. In Section II, the basic principle of the FDM is presented. Then we describe how the ACA is combined with the FDM in detail. In Section III, some numerical results about the bistatic radar cross section (RCS) are given to verify the efficiency and accuracy of the new method. Finally, conclusions are drawn in Section IV.

II. FORMULATIONS

A. Basic Principles of the FDM

For perfect electric conducting (PEC) targets, the equivalent dipole method (EDM) [13-14] views each RWG element as a small dipole and the mutual impedance is replaced by the interaction between two dipoles when the distance of the two dipoles is beyond a appropriate threshold distance (typically 0.2 λ ~0.5 λ). Considering two well-separated dipoles (the *m*th dipole and the *n*th dipole), the relevant impedance element for electric field integral equation (EFIE) and magnetic field integral equation (MFIE) can be calculated by [13-14]

$$Z_{mn}^{E} = jk\eta \mathbf{m}_m \cdot \bar{\mathbf{G}}(\mathbf{R}) \cdot \mathbf{m}_n \tag{1}$$

$$Z_{mn}^{M} = jk\eta \mathbf{m}'_m \cdot \mathbf{G}(\mathbf{R}) \times \mathbf{m}_n \tag{2}$$

where

$$\bar{\mathbf{G}}(\mathbf{R}) = \frac{e^{-jkR}}{4\pi R}\left[\bar{\mathbf{I}}\left(1+\frac{1}{jkR}+\frac{1}{(jkR)^2}\right) - \hat{\mathbf{R}}\hat{\mathbf{R}}\left(1+\frac{3}{jkR}+\frac{3}{(jkR)^2}\right)\right] \tag{3}$$

$$\mathbf{G}(\mathbf{R}) = \frac{e^{-jkR}}{4\pi R}\left(1+\frac{1}{jkR}\right)\hat{\mathbf{R}} \tag{4}$$

In (1)~(4), $\mathbf{m}_m = l_m(\mathbf{r}_m^{c-} - \mathbf{r}_m^{c+})$ and $\mathbf{m}_n = l_n(\mathbf{r}_n^{c-} - \mathbf{r}_n^{c+})$ are the equivalent dipole moments of the *m*th and *n*th RWG elements. $\mathbf{m}'_m = \mathbf{m}_m \times \hat{\mathbf{n}}_m$. $\mathbf{r}_m^{c\pm}(\mathbf{r}_n^{c\pm})$ is the position vector of the centroid of two adjacent triangular patches $T_m^{\pm}(T_n^{\pm})$, and $l_m(l_n)$ is the length of the common edge of $T_m^{\pm}(T_n^{\pm})$. $\hat{\mathbf{n}}_m = (\hat{\mathbf{n}}_m^{+} + \hat{\mathbf{n}}_m^{-})\big/\left|\hat{\mathbf{n}}_m^{+} + \hat{\mathbf{n}}_m^{-}\right|$ is the average normal vector, and $\hat{\mathbf{n}}_m^{\pm}$ represent the unit normal vectors of $T_m^{\pm}$. $\mathbf{r}_n = (\mathbf{r}_n^{c+} + \mathbf{r}_n^{c-})/2$ and $\mathbf{r}_m = (\mathbf{r}_m^{c+} + \mathbf{r}_m^{c-})/2$ respectively represent the position vectors of the *n*th and *m*th dipoles' centers (see Fig. 1). $\mathbf{R} = \mathbf{r}_{mn} = \mathbf{r}_m - \mathbf{r}_n$, $R = |\mathbf{R}|$, $\hat{\mathbf{R}} = \mathbf{R}/R$. η and k are the impedance and wavenumber of the free space.

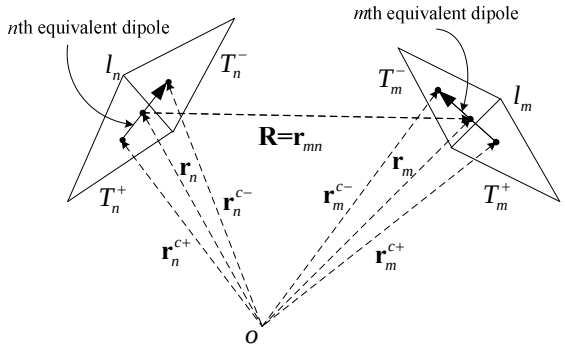

Fig. 1. Geometry of the *m*th and *n*th RWG elements and their equivalent dipole models [16].

It can be seen from (1) and (2) that the calculation of mutual impedance elements of both EFIE and MFIE in the EDM is very simple. However, it don't change the memory cost and matrix-solve time. The fast dipole method (FDM) [16-17] can mitigate this problem. In the FDM, the target is grouped with equally sized cubes, then all dipoles are assigned to individual cubes. The FDM is used in those far-group pairs. We use $D(i,j) = \max\{|x_i - x_j|, |y_i - y_j|, |z_i - z_j|\}/\Delta$ to define the distance between two groups i and j , in which (x_i, y_i, z_i) and (x_j, y_j, z_j) are the coordinates of the centroid of group i and group j , Δ is the side length of the group. A given integer D_b ($D_b \geqslant 1$) is used to decide if the two groups are far-group pair. If $D(i,j) > D_b$, the two groups are a far-group pair. It can be found that the FDM will give more accurate solutions with the increment of D_b , so D_b can be used to control the accuracy of the FDM.

Now, we consider two dipoles *m* and *n* that respectively belongs to group j and i , and suppose the two groups are a far-group pair. The impedance element can be represented as (1) and (2) for EFIE and MFIE. The distance between the two dipoles can be written as

$$\mathbf{R} = \mathbf{r}_{ji} + \mathbf{r}_{mj} - \mathbf{r}_{ni} = \mathbf{r}_{mp} - \mathbf{r}_{np} \tag{5}$$

where $\mathbf{r}_{ji} = \mathbf{r}_{o_j} - \mathbf{r}_{o_i}$, $\mathbf{r}_{mj} = \mathbf{r}_m - \mathbf{r}_{o_j}$, $\mathbf{r}_{ni} = \mathbf{r}_n - \mathbf{r}_{o_i}$. $\mathbf{r}_{mp} = \mathbf{r}_m - \mathbf{r}_p$, $\mathbf{r}_{np} = \mathbf{r}_n - \mathbf{r}_p$, $\mathbf{r}_p = \left(\mathbf{r}_{o_j} + \mathbf{r}_{o_i}\right)/2$. $\mathbf{r}_{o_i}$ and

$\mathbf{r}_{o_j}$ are the center positions of group i and j shown in Fig. 2.

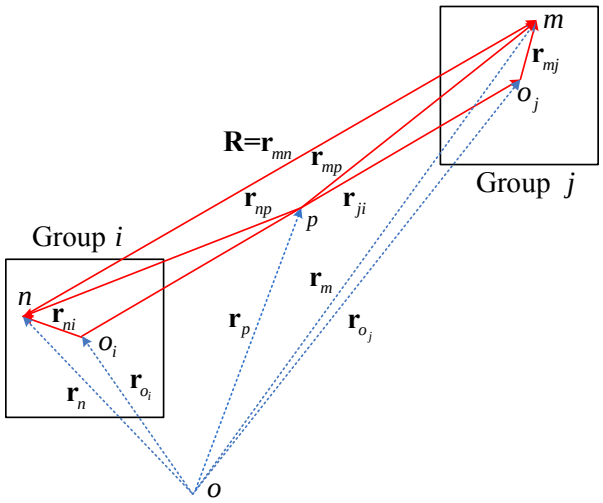

Fig. 2. The mth and nth RWG elements and the groups they belong to [16].

R^{α} (α =1,-1,-2,-3) in (3) and (4) can be expanded using the Taylor series as [17]

$$\begin{aligned} R^{\alpha} &= \left|\mathbf{r}_{ji}+\mathbf{r}_{mj}-\mathbf{r}_{ni}\right|^{\alpha} \\ &= r_{ji}^{\alpha}\left[1+\left(\frac{2\hat{\mathbf{r}}_{ji}\cdot\mathbf{r}_{mj}}{r_{ji}}+\frac{r_{mj}^2}{r_{ji}^2}\right)+\left(\frac{2\hat{\mathbf{r}}_{ij}\cdot\mathbf{r}_{ni}}{r_{ij}}+\frac{r_{ni}^2}{r_{ij}^2}\right)-\frac{2\mathbf{r}_{mj}\cdot\mathbf{r}_{ni}}{r_{ji}^2}\right]^{\frac{\alpha}{2}} \\ &\approx R_m^{(\alpha)}+R_n^{(\alpha)} \end{aligned} \tag{6}$$

where

$$R_m^{(\alpha)} = r_{ji}^{\alpha}\left[\frac{1}{2}+\alpha\left(\frac{\hat{\mathbf{r}}_{ji}\cdot\mathbf{r}_{mj}}{r_{ji}}+\frac{r_{mj}^2+(\alpha-2)\left(\hat{\mathbf{r}}_{ji}\cdot\mathbf{r}_{mj}\right)^2}{2r_{ji}^2}\right)\right] \tag{7}$$

$$R_n^{(\alpha)} = r_{ij}^{\alpha}\left[\frac{1}{2}+\alpha\left(\frac{\hat{\mathbf{r}}_{ij}\cdot\mathbf{r}_{ni}}{r_{ij}}+\frac{r_{ni}^2+(\alpha-2)\left(\hat{\mathbf{r}}_{ij}\cdot\mathbf{r}_{ni}\right)^2}{2r_{ij}^2}\right)\right] \tag{8}$$

The dyad $\hat{\mathbf{R}}\hat{\mathbf{R}}$ in (3) can be approximated as [17]

$$\begin{aligned} \hat{\mathbf{R}}\hat{\mathbf{R}} &\approx \frac{1}{r_{ji}^2}\left[\mathbf{r}_{ji}\mathbf{r}_{ji}+(\mathbf{s}_m-\mathbf{s}_n)\mathbf{r}_{ji}+\mathbf{r}_{ji}(\mathbf{s}_m-\mathbf{s}_n)\right] \\ &= \overline{\mathbf{T}}_m+\overline{\mathbf{T}}_n \end{aligned} \tag{9}$$

in which

$$\overline{\mathbf{T}}_m = \frac{1}{r_{ji}^2}\left[\frac{1}{2}\mathbf{r}_{ji}\mathbf{r}_{ji}+\mathbf{s}_m\mathbf{r}_{ji}+\mathbf{r}_{ji}\mathbf{s}_m\right] \tag{10}$$

$$\overline{\mathbf{T}}_n = \frac{1}{r_{ij}^2}\left[\frac{1}{2}\mathbf{r}_{ij}\mathbf{r}_{ij}+\mathbf{s}_n\mathbf{r}_{ij}+\mathbf{r}_{ij}\mathbf{s}_n\right] \tag{11}$$

$$\mathbf{s}_m = \mathbf{r}_{mj}-\mathbf{r}_{mj}\cdot\hat{\mathbf{r}}_{ji}\hat{\mathbf{r}}_{ji} \tag{12}$$

$$\mathbf{s}_n = \mathbf{r}_{ni}-\mathbf{r}_{ni}\cdot\hat{\mathbf{r}}_{ij}\hat{\mathbf{r}}_{ij} \tag{13}$$

Substituting (6) (α =1,-1,-2,-3) and (9) into (1), and substituting (6) (α =1,-2,-3) and (5) into (2), the impedance element in the FDM for EFIE and MFIE can be obtained.

$$\begin{aligned} Z_{mn}^{E} &\approx \frac{jk\eta}{4\pi}\mathbf{M}_m\cdot\left[\overline{\mathbf{I}}(A_m+A_n)-(\overline{\mathbf{T}}_m+\overline{\mathbf{T}}_n)(B_m+B_n)\right]\cdot\mathbf{M}_n \\ &= \frac{jk\eta}{4\pi}\Big[\left(A_m\mathbf{M}_m-B_m\mathbf{M}_m\cdot\overline{\mathbf{T}}_m\right)\cdot\mathbf{M}_n \\ &\quad +\mathbf{M}_m\cdot\left(A_n\mathbf{M}_n-B_n\overline{\mathbf{T}}_n\cdot\mathbf{M}_n\right)-\left(\mathbf{M}_m\cdot\overline{\mathbf{T}}_m\right)\cdot\left(B_n\mathbf{M}_n\right) \\ &\quad -\left(B_m\mathbf{M}_m\right)\cdot\left(\overline{\mathbf{T}}_n\cdot\mathbf{M}_n\right)\Big] \end{aligned} \tag{14}$$

$$\begin{aligned} Z_{mn}^{M} &\approx \frac{jk\eta}{4\pi}\mathbf{M}'_m\cdot(C_m+C_n)\left(\mathbf{r}_{mp}-\mathbf{r}_{np}\right)\times\mathbf{M}_n \\ &= \frac{jk\eta}{4\pi}\Big[\left(C_m\mathbf{M}'_m\times\mathbf{r}_{mp}\right)\cdot\mathbf{M}_n \\ &\quad +\left(\mathbf{M}'_m\times\mathbf{r}_{mp}\right)\cdot\left(C_n\mathbf{M}_n\right) \\ &\quad +\left(C_m\mathbf{M}'_m\right)\cdot\left(\mathbf{M}_n\times\mathbf{r}_{np}\right) \\ &\quad +\mathbf{M}'_m\cdot\left(C_n\mathbf{M}_n\times\mathbf{r}_{np}\right)\Big] \end{aligned} \tag{15}$$

where

$$A_u = R_u^{(-1)}+(jk)^{-1}R_u^{(-2)}+(jk)^{-2}R_u^{(-3)} \tag{16}$$

$$B_u = R_u^{(-1)}+3(jk)^{-1}R_u^{(-2)}+3(jk)^{-2}R_u^{(-3)} \tag{17}$$

$$C_u = R_u^{(-2)}+(jk)^{-1}R_u^{(-3)} \tag{18}$$

$$\mathbf{M}_u = \mathbf{m}_u e^{-jkR_u^{(1)}} \tag{19}$$

$$\mathbf{M}'_u = \mathbf{m}'_u e^{-jkR_u^{(1)}} \tag{20}$$

for $u=m,n$

Now we discuss how the FDM can efficiently calculate the MVPs for a far-group pair (such as group j and i). We suppose the two groups contain N_j and N_i dipoles, respectively. For a iterative solver such as GMRES, the MVP between far groups j and i

$$\mathbf{V}_j = \mathbf{Z}_{ji}\mathbf{I}_i \tag{21}$$

need be computed, where $\mathbf{Z}_{ji}$ are the impedance submatrix between groups j and i, whose size is $N_j\times N_i$, $\mathbf{I}_i$ with a size of $N_i\times 1$ is the current subvector, $\mathbf{V}_j$ with a size of $N_j\times 1$ is the result of $\mathbf{Z}_{ji}\mathbf{I}_i$. The complexity of (21) is $O(N_iN_j)$. When

the FDM is used to calculate these interactions between groups j and i, an element v_m of $\mathbf{V}_j$ for EFIE and MFIE can be approximatively represented as follows.

$$\begin{aligned} v_m^E &= \sum_{n=1}^{N_i} Z_{mn}^E I_n \\ &\approx \frac{jk\eta}{4\pi}\Bigg[\left(A_m\mathbf{M}_m - B_m\mathbf{M}_m\cdot\bar{\mathbf{T}}_m\right)\cdot\sum_{n=1}^{N_i}\mathbf{M}_n I_n \\ &\quad +\mathbf{M}_m\cdot\sum_{n=1}^{N_i}\left(A_n\mathbf{M}_n - B_n\bar{\mathbf{T}}_n\cdot\mathbf{M}_n\right)I_n \\ &\quad -\left(\mathbf{M}_m\cdot\bar{\mathbf{T}}_m\right)\cdot\sum_{n=1}^{N_i}\left(B_n\mathbf{M}_n\right)I_n \\ &\quad -\left(B_m\mathbf{M}_m\right)\cdot\sum_{n=1}^{N_i}\left(\bar{\mathbf{T}}_n\cdot\mathbf{M}_n\right)I_n\Bigg] \end{aligned} \tag{22}$$

$$\begin{aligned} v_m^M &= \sum_{n=1}^{N_i} Z_{mn}^M I_n \\ &\approx \frac{jk\eta}{4\pi}\Bigg[\left(C_m\mathbf{M}'_m\times\mathbf{r}_{mp}\right)\cdot\sum_{n=1}^{N_i}\mathbf{M}_n I_n \\ &\quad +\left(\mathbf{M}'_m\times\mathbf{r}_{mp}\right)\cdot\sum_{n=1}^{N_i}\left(C_n\mathbf{M}_n\right)I_n \\ &\quad +\left(C_m\mathbf{M}'_m\right)\cdot\sum_{n=1}^{N_i}\left(\mathbf{M}_n\times\mathbf{r}_{np}\right)I_n \\ &\quad +\mathbf{M}'_m\cdot\sum_{n=1}^{N_i}\left(C_n\mathbf{M}_n\times\mathbf{r}_{np}\right)I_n\Bigg] \end{aligned} \tag{23}$$

Now we consider a term in (22) as an example to illustrate how the FDM works. It can be found that

$$\left(A_m\mathbf{M}_m - B_m\mathbf{M}_m\cdot\bar{\mathbf{T}}_m\right)\cdot\sum_{n=1}^{N_i}\mathbf{M}_n I_n \tag{24}$$

achieves the separation of *m* and *n*. Therefore, the result $\sum_{n=1}^{N_i}\mathbf{M}_n I_n$ is independent of *m*. For different dipole *m* in group *j*, $\sum_{n=1}^{N_i}\mathbf{M}_n I_n$ can be reused, so it only need be calculated once. All other terms in (22) and (23) can be handled in the same way. Thus the complexity of (21) is reduced to $O(N_i + N_j)$ by the FDM.

B. The ACA-FDM

It is easy to know that the error brought by the FDM is decreasing with the increment of D_b. However, with the increase in D_b the near region increases quickly, which will increase memory and CPU time requirement. In this article, the adaptive cross approximation (ACA) [8] is employed in the near region to mitigate this problem. The ACA algorithm is a matrix decomposition algorithm which only requires partial impedance elements of original matrices and easy to implement, which can be efficiently calculated by the EDM.

Considering two near groups such as group i and group j $(1 < D(i,j) \le D_b)$ which include N_i and N_j dipoles, respectively. The interactions $\mathbf{Z}_{ji}$ between the two groups can be approximated by the ACA as

$$\mathbf{Z}_{ji} \approx \mathbf{U}_{ji}\mathbf{V}_{ji} \tag{25}$$

where *r* denotes the effective rank of the submatrix $\mathbf{Z}_{ji}$. $\mathbf{U}_{ji}$ is a matrix of size $N_j \times r$, and $\mathbf{V}_{ji}$ is a matrix of size $r \times N_i$. The goal of the ACA is to achieve error matrix

$$\left\|\mathbf{R}_{ji}\right\|_F = \left\|\mathbf{Z}_{ji} - \mathbf{U}_{ji}\mathbf{V}_{ji}\right\|_F \le \varepsilon\left\|\mathbf{Z}_{ji}\right\|_F \tag{26}$$

where ε is a given tolerance, and $\|\bullet\|_F$ represents the matrix Frobenus norm. The accuracy of the ACA can be easily controlled by a given tolerance ε. According to [8], a tolerance of 10^{-2} can give accurate results, which is used in the ACA region in this paper.

The detail of the ACA algorithm [8] is presented as follows.

□ Initialization $\tilde{\mathbf{R}} = 0$, $\left\|\tilde{\mathbf{Z}}^{(0)}\right\|^2 = 0$, $k = 1$.

□ Find I_k : if $(k = 1)$ $I_k = 1$; else $I_k : \left|\tilde{\mathbf{R}}(I_k, J_{k-1})\right| = \max_i\left(\left|\tilde{\mathbf{R}}(i, J_{k-1})\right|\right)$, $i \ne I_1, \cdots, I_{k-1}$.

□ $\tilde{\mathbf{R}}(I_k,:) = \mathbf{Z}(I_k,:) - \sum_{l=1}^{k-1}(\mathbf{u}_l)_{I_k}\mathbf{v}_l$.

□ Find J_k : $\left|\tilde{\mathbf{R}}(I_k, J_k)\right| = \max_j\left(\left|\tilde{\mathbf{R}}(I_k, j)\right|\right)$, $j \ne J_1, \cdots, J_{k-1}$.

□ $\mathbf{v}_k = \tilde{\mathbf{R}}(I_k,:)/\tilde{\mathbf{R}}(I_k, J_k)$.

□ $\tilde{\mathbf{R}}(:, J_k) = \mathbf{Z}(:, J_k) - \sum_{l=1}^{k-1}(\mathbf{v}_l)_{J_k}\mathbf{u}_l$.

□ $\mathbf{u}_k = \tilde{\mathbf{R}}(:, J_k)$.

□ $\left\|\tilde{\mathbf{Z}}^{(k)}\right\|^2 = \left\|\tilde{\mathbf{Z}}^{(k-1)}\right\|^2 + 2\sum_{j=1}^{k-1}\left|\mathbf{u}_j^T\mathbf{u}_k\right|\left|\mathbf{v}_j^T\mathbf{v}_j\right| + \left\|\mathbf{u}_k\right\|^2\left\|\mathbf{v}_k\right\|^2$.

□ Check convergence: if $(\|\mathbf{u}_k\|\|\mathbf{v}_k\| \le \varepsilon\|\tilde{\mathbf{Z}}^{(k)}\|)$, end iteration; else $k = k+1$ and goto □.

The MVP related to the two near groups *j* and *i* can be approximatively represented as

$$\mathbf{Z}_{ji}\mathbf{I}_i \approx \mathbf{U}_{ji}\left(\mathbf{V}_{ji}\mathbf{I}_i\right) \tag{27}$$

Clearly, the complexity of (27) is $O(r(N_i + N_j))$. Moreover, $\mathbf{U}_{ji}$ and $\mathbf{V}_{ji}$ are stored instead of $\mathbf{Z}_{ji}$, so the complexity of memory requirement is also reduced to $O(r(N_i + N_j))$.

In ACA-FDM, the ACA and the FDM are used to deal with the near-group pairs and the far-group pairs, respectively. Thus both near-group pairs and far-group pairs can be efficiently calculated in the ACA-FDM. Compared with the conventional FDM, the performance of the near-group interactions are improved by the ACA.

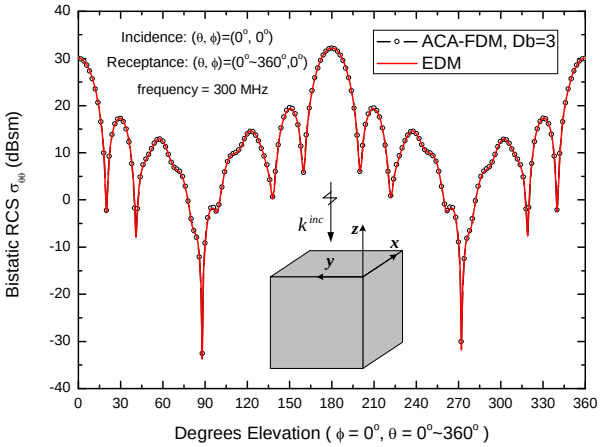

Fig. 3. Bistatic RCSs of a 3 m×3 m×3 m PEC cube.

III. NUMERICAL RESULTS

In this section, the ACA-FDM is implemented in the RCS calculations. All the simulations are performed on a personal computer with the Intel(R) Pentium(R) Dual-Core CPU E5500 with 2.8 GHz (only one core is used) and 2.0 GB RAM. The combined field integral equation (CFIE) (combination parameter is 0.5) is used. The GMRES iterative solver is employed to obtain an identical residual error ≤ 0.01. The block diagonal preconditioner (BDP) is used in all the simulations. All the targets are discretized into triangular patches with an average edge length of 0.1λ. In this paper, the threshold distance of the EDM is chosen as $0.2\,\lambda$. All the objects are illuminated by a $\hat{\mathbf{x}}$-polarized plane wave with the incident direction of $(\theta,\phi) = (0^\circ, 0^\circ)$

First we consider the scattering problem of a PEC cube with side length of 2.5 m. The cube is divided into 12228 triangular patches, and the total number of unknowns is 18342. All the unknowns are divided into 218 nonempty groups and the size of each group is $0.45\,\lambda$. Figure 3 gives the bistatic RCSs for $\theta\theta$ polarization calculated by the ACA-FDM (D_b=3) and the EDM. Results show good agreement.

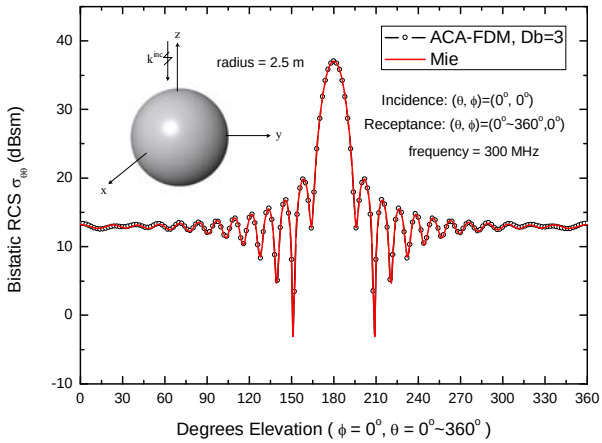

Fig. 4. Bistatic RCSs of a PEC sphere of radius 2.5 m.

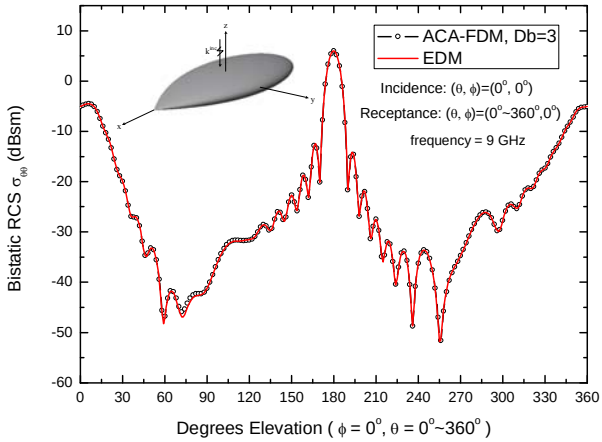

Fig. 5. Bistatic RCSs of a 252.3744-mm PEC NASA almond.

The second problem is a PEC sphere with radius 3 m. The sphere is meshed into 19260 triangular patches and there are total 28890 unknowns. All the unknowns are divided into 409 nonempty groups and the size of each group is $0.55\,\lambda$. The bistatic RCSs in $\theta\theta$ polarization are shown in Fig. 4. The result obtained by the ACA-FDM (D_b=3) agrees well with the Mie series solution, which is exact and used as a reference.

Finally, the bistatic RCSs of a 252.3744-mm PEC NASA almond are calculated. The almond is divided into 8808 triangular patches and the

number of unknowns is 13212. Totally 102 nonempty groups with the size of 0.65 λ are obtained. The bistatic RCS in $\theta\theta$ polarization calculated by the ACA-FDM (D_b=3) is compared with the EDM shown in Fig. 5.

Table 1: Comparison of CPU time and memory cost for different D_b values

Problem 1: cube		
D_b	FDM/ACA-FDM	
	Time (s)	RAM (MB)
1	61/61	135/135
2	75/66	363/194
3	97/73	706/270
Problem 2: sphere		
D_b	FDM/ACA-FDM	
	Time (s)	RAM (MB)
1	159/159	280/280
2	188/166	745/386
3	236/182	1434/523
Problem 3: almond		
D_b	FDM/ACA-FDM	
	Time (s)	RAM (MB)
1	38/38	229/229
2	57/42	504/273
3	76/45	775/310

The memory requirements and CPU time for the simulations above are summarized in Table 1. From Table 1, it can be found that the ACA-FDM saves CPU time and memory requirement than the conventional FDM, when D_b (>1) is chosen as the same value for the two methods. When D_b=1, the ACA-FDM is the same as the conventional FDM, because the ACA algorithm is only used to handle the nonadjacent groups. As shown in Fig. 3~5, we can find that the CFIE (combination parameter is 0.5) solved by the ACA-FDM (D_b=3) can give good RCS solutions for the three examples. However, it is worth mentioning that the stricter criterion D_b of the ACA-FDM may be required when more complex or larger targets are calculated, or when larger group size is chosen.

IV. CONCLUSION

In this article, a hybrid ACA-FDM is implemented to accelerate solving the electromagnetic scattering from PEC targets. In the ACA-FDM, the ACA and the FDM are used to deal with the near-group pairs and the far-group pairs, respectively. Profiting from the use of ACA algorithm in the near region, the ACA-FDM saves memory and CPU time than the FDM when the criteria for the far region becomes stricter.

ACKNOWLEDGMENT

The work was supported by the National Nature Science Foundation of China under Grant No. 61071019, the Funding of Jiangsu Innovation Program for Graduate Education under Grant No. CXZZ11_0229, and the Fundamental Research Funds for the Central Universities.

REFERENCES

[1] J. M. Song and W. C. Chew, "Multilevel Fast-Multipole Algorithm for Solving Combined Field Integral Equations of Electromagnetic Scattering," *Microwave Opt. Technol. Lett.*, vol. 10, no. 1, pp. 14-19, 1995.

[2] J. M. Song, C. C. Lu, and W. C. Chew, "Multilevel Fast Multipole Algorithm for Electromagnetic Scattering by Large Complex Objects," *IEEE Trans. Antennas Propagat.*, vol. 45, no. 10, pp. 1488-1493, 1997.

[3] E. Bleszynski, M. Bleszynski, and T. Jaroszewicz, "AIM: Adaptive Integral Method for Solving Large-scale Electromagnetic Scattering and Radiation Problems," *Radio Sci*, vol. 31, no. 5, pp. 1225-1251, 1996.

[4] C. F. Wang, F. Ling, J. Song, and J.-M. Jin, "Adaptive Integral Solution of Combined Field Integral Equation," *Microw. Opt. Technol. Lett.*, vol. 19, no. 5, pp. 321-328, 1998.

[5] J. K. White, J. R. Phillips and T. Korsmeyer, "Comparing Precorrected-FFT Method and Fast Multipole Algorithms for Solving Three-dimensional Potential Integral Equations," *Proc Cocrado Conf Iterative Methods, Proceedings*, 1994.

[6] J. R. Phillips and J. K. White, "A Precorrected-FFT Method for Electrostatic Analysis of Complicated 3-D Structures," *IEEE Trans. Computer-Adided Design Integr Circuits Syst.*, vol. 16, no. 10, pp. 1059-1072, 1997.

[7] M. Bebendorf, "Approximation of Boundary Element Matrices," *Numer. Math*, vol. 86, no. 4, pp. 565-589, 2000.

[8] K. Zhao, M. N. Vouvakis, and J.-F. Lee, "The Adaptive Cross Approximation Algorithm for Accelerated Method of Moments Computations of EMC," *IEEE Trans. Electromagn. Compat.*, vol. 47, no. 4, pp. 763-773, 2005.

[9] Z. Liu, R. Chen, J. Chen, Z. Fan, "Using Adaptive Cross Approximation for Efficient Calculation of Monostatic Scattering with Multiple Incident Angles," *Applied Computational Electromagnetics Society (ACES) Journal*, vol. 26, no. 4, pp. 325-333, 2011.

[10] R. S. Chen, Z. H. Fan, Y. Y. An, M. M. Zhu, K. W. Leung, "Modified Adaptive Cross Approximation Algorithm for Analysis of Electromagnetic Problems," *Applied Computational Electromagnetics Society (ACES) Journal*, vol. 26, no. 2, pp. 160-169, 2011.

[11] M. Chen, R. S. Chen, X. Q. Hu, "Augmented MLFMM for Analysis of Scattering from PEC Object with Fine Structures," *Applied Computational Electromagnetics Society (ACES) Journal*, vol. 26, no. 5, pp. 418-428, 2011.

[12] T. Wan, R. Chen, X. Hu, Y. Chen, Y. Shen, "Efficient Direct Solution of EFIE for Electrically Large Scattering Problems using H-LDLT and PE Basis Function," *Applied Computational Electromagnetics Society (ACES) Journal*, vol. 26, no. 7, pp. 561-571, July 2011.

[13] J. Yeo, S. Koksoy, V. V. S. Prakash, and R. Mittra, "Efficient Generation of Method of Moments Matrices using the Characteristic Function Method," *IEEE Trans. Antennas Propag.*, vol. 52, no. 12, pp. 3405-3410, 2004.

[14] J. Yuan, C. Gu and G. Han, "Efficient Generation of Method of Moments Matrices using Equivalent Dipole-moment Method," *IEEE Antennas and Wireless Propag. Lett.*, vol. 8, pp. 716-719, 2009.

[15] S. M. Rao, D. R. Wilton, and A. W. Glisson, "Electromagnetic Scattering by Surfaces of Arbitrary Shape," *IEEE Trans. Antennas Propag*., vol. 30, no. 3, pp. 409-418, 1982.

[16] X. Chen, C. Gu, Z. Niu and Z. Li, "Fast Dipole Method for Electromagnetic Scattering from Perfect Electric Conducting Targets," *IEEE Trans. Antennas Propag*., vol. 60, no. 2, pp. 1186-1191, 2012.

[17] X. Chen, Z. Li, Z. Niu, and C. Gu, "Analysis of Electromagnetic Scattering from PEC Targets using Improved Fast Dipole Method," *Journal of Electromagnetic Waves and Applications*, vol. 25, no. 16, pp. 2254-2263, 2011.